Journal of
Applied Remote Sensing

RemoteSensing.SPIEDigitalLibrary.org

Unbiased-average minimum biased diffusion speckle denoising approach for synthetic aperture radar images

Bing Sun
Jie Chen
Eric Tovar
Zhijun Qiao

SPIE.

Unbiased-average minimum biased diffusion speckle denoising approach for synthetic aperture radar images

Bing Sun,[a] Jie Chen,[a,*] Eric Tovar,[b] and Zhijun Qiao[b]

[a]Beihang University, School of Electronics and Information Engineering, Department of Information and Communication Engineering, 37 Xueyuan Road, Haidian District, Beijing 100191, China

[b]University of Texas-Pan America, Department of Mathematics, 1201 West University Drive, Edinburg, Texas 78539, United States

Abstract. Means of synthetic aperture radar (SAR) images represent the radiation densities of scenes, and the preservation of means is significant in speckle denoising for the application of SAR images. We provide an improved scheme of the minimum biased diffusion (MinBAD) algorithm for speckle denoising using partial differential equations. Considering the characteristics of SAR speckle and the radiation accuracy for postprocessing needs, several improvements such as normalization, homomorphic transformation, and average-preserving processing are introduced into the MinBAD algorithm. Besides the equivalent number of looks and edge preserving index, a new index, radiation accuracy error, is defined to evaluate the denoising effect. Experimental results for both artificial images and real SAR images are used to validate the performance of the proposed unbiased-average MinBAD speckle reducing approach. [DOI: 10.1117/1.JRS.9.095081]

Keywords: partial differential equations; speckle denoising; minimum biased diffusion; unbiased-average; radiation accuracy error.

Paper 15071 received Jan. 26, 2015; accepted for publication Apr. 2, 2015; published online Apr. 28, 2015.

1 Introduction

Speckle denoising for synthetic aperture radar (SAR) images has been a critical and difficult problem for several decades. Current typical denoising approaches can be classified into two categories: temporal domain filtering and transform domain filtering. Representative temporal domain filters include the average filter, median filter, Lee filter,[1] maximum *a posteriori*-class filters,[2–4] and so on; and representative transform domain filters include the low-pass filter, wavelet-based filter,[5–8] and so on. Due to the high-frequency characteristics of noise and edges which are difficult to distinguish, the overall effect of low-pass filters is not prominent. A wavelet transform, which introduces multiple scale subimages, will improve the filtering effect. Over the last few years, partial differential equation (PDE)-based denoising methodologies[9–13] have become an important type of denoising. Typical algorithms include the Perona–Malik (PM) algorithm[9] and its variants. The main advantage of these anisotropic diffusion algorithms is to denoise while minimizing the loss of information on the edges which yields satisfactory results.

Minimum biased diffusion (MinBAD) is a very useful approach, introduced by Kim et al.[14–17] Excellent denoising abilities have been illustrated on artificial scenes and standard test images such as the Lena image. Denoising abilities also fit to optical images very well. However, SAR images have multiplicative noise and a large dynamic range. Denoising is affected by the direct

*Address all correspondence to: Jie Chen, E-mail: chenjie@buaa.edu.cn

MinBAD method. Additionally, preservation of the means of SAR subimages is very important for applications, such as target detection, classification, and so on. Because the means represent the radiation densities of the scene in SAR images, changing the means affects the results after denoising. Most nonlinear filters, including median filters, MinBAD filters, and so on, will change the energy and the means of subimages while denoising, and the radiation accuracy is affected too. The previously mentioned speckle reducing methods mainly aim to decrease the noise level, which is evaluated by the equivalent number of looks (ENL) and edge preserving ability. We have found that edge preserving and radiation accuracy are more significant than ENL when the ENL is at a high level for actual applications of SAR images.

Our aim is to find an approach with good edge and radiation preserving abilities while denoising. This paper develops the MinBAD method for SAR image speckle denoising. The characteristics and postprocessing demands of SAR images are also considered. The improved steps include normalization, homomorphic transform and inverse transform, and average-preserving processing.

The paper is organized as follows. In Sec. 2, the classic denoising PDEs models are presented, including PM and MinBAD models. Section 3 introduces the unbiased-average MinBAD approach schemes, and explains the three improved steps and the key numerical time parameters for locally one-dimensional (1-D) methods. In Sec. 4, three evaluation indices including ENL, edge preserving index (EPI), and radiation accuracy error (RAE) are defined. We then present the experimental results for both artificial and real SAR images which validate the performance of the proposed unbiased-average MinBAD speckle denoising approach. Finally, a conclusion is given in Sec. 5.

2 Preliminaries

Anisotropic diffusion PDEs have been a popular tool for denoising since the PM model was introduced in 1990.[9] In this section, we briefly introduce the simplest linear diffusion PDEs, PM anisotropic diffusion PDEs, and variants, and the MinBAD PDEs with some key parameters.

2.1 *Perona–Malik and Its Variants*

Linear filtering operators can be expressed by the linear diffusion form

$$\frac{\partial u}{\partial t} = \nabla \cdot D(x)\nabla u, \tag{1}$$

where $x \in \Omega$ and Ω is the space domain of the image, and $u(x, t = 0) = u^0(x)$ is the noised image and the initial diffusion image. Clearly, the average operator satisfies this model. The linear diffusion model unavoidably smears sharp edges embedded in $u^0(x)$ while filtering out noise. To remedy this shortcoming, Perona and Malik allowed the diffusivity coefficient D to be adapted to the image itself instead of being prefixed:

$$D = D(x, u, \nabla u). \tag{2}$$

In general, the desirable diffusivity coefficient D must qualitatively attain edge selectivity. That is, D is large when $|\nabla u|$ is small on intraregions and D is large when $|\nabla u|$ is large on intraregions or near edges. Then, the following nonlinear diffusion model can be defined by

$$\frac{\partial u}{\partial t} = \nabla \cdot [g(|\nabla u|)\nabla u], \tag{3}$$

where $g(x)$ is the diffusion function, and $g(x) \to 0$ as $x \to \infty$. Usually, one of the following expressions may be chosen

$$g(x) = \frac{1}{1 + (\frac{x}{k})^2} \tag{4}$$

or

$$g(x) = \exp\left\{-\left(\frac{x}{k}\right)^2\right\}, \tag{5}$$

where k is the threshold of the image gradient magnitude. This traditional anisotropic diffusion approach can filter the additive noise and preserve the edges of the image, but the actual challenge is how to robustly compute the diffusion coefficient D or the threshold k at the very beginning of the initial value problem if u_0 is highly oscillatory. Another challenge is being able to distinguish speckle noises and edges for SAR images.

However, Perona and Malik presented an anisotropic diffusion approach, and this nonlinear diffusion model has been recently developed. Speckle reducing anisotropic diffusion[13] is a good approach as well. Also, the general adaptive speckle filters such as the Lee filter and Frost filter[18] are proven to be some of the forms of the PM model in Ref. 13.

2.2 *Minimum Biased Anisotropic Diffusion Approach*

In Refs. 14–17, Kim et al. presented an anisotropic diffusion model

$$\frac{\partial u}{\partial t} = |\nabla u| \nabla \cdot \left(\frac{\nabla u}{\|\nabla u\|}\right), \tag{6}$$

where $\|\nabla u\| = \sqrt{u_x^2 + u_y^2}$ and $|\nabla u|$ is the minimum biased anisotropic diffusion (MinBAD) term, and can be calculated by the following schemes. Given a grid point (i, j), let (l, m) be one of the eight neighboring points. Let

$$D_{(i,j)}^{(l,m)}(u) = \frac{|u_{i,j} - u_{l,m}|}{\sqrt{(i-l)^2 + (j-m)^2}}, \tag{7}$$

where $(l, m) \in [i-1, i+1] \times [j-1, j+1]$, $(l, m) \neq (i, j)$. Let the above eight differences be ordered as

$$D_{(i,j)}^{(l_1,m_1)}(u) \leq D_{(i,j)}^{(l_2,m_2)}(u) \leq \cdots \leq D_{(i,j)}^{(l_8,m_8)}(u), \tag{8}$$

where (l_k, m_k), $k = 1,2,\ldots,8$ represent the eight neighboring points. Then, the essentially minimum-biased finite-difference scheme for $|\nabla u|$ at (i, j) is defined as

$$|\nabla u|_{i,j} = \sqrt{[D_{(i,j)}^{(l_1,m_1)}(u)]^2 + [D_{(i,j)}^{(l_2,m_2)}(u)]^2}, \tag{9}$$

and the minimum slope (Min-Slope) scheme is defined as

$$|\nabla u|_{i,j} = D_{(i,j)}^{(l_1,m_1)}(u). \tag{10}$$

The MinBAD and Min-Slope scheme can be understood as follows: (1) for a flat area inside of the target or the background, the eight differences are very small, and one iteration will keep most of the information; (2) for the edge lines, at least two of the eight differences are very small. Then after one iteration, the edge will preserve; and (3) for single noise points, almost eight differences are sufficiently large, and the noise will be removed quickly after one iteration.

The denoising results were excellent after a few iterations. Figure 1 shows one set of results filtered by the MinBAD method. Figures 1(a), 1(c), and 1(e) are images with random pulse

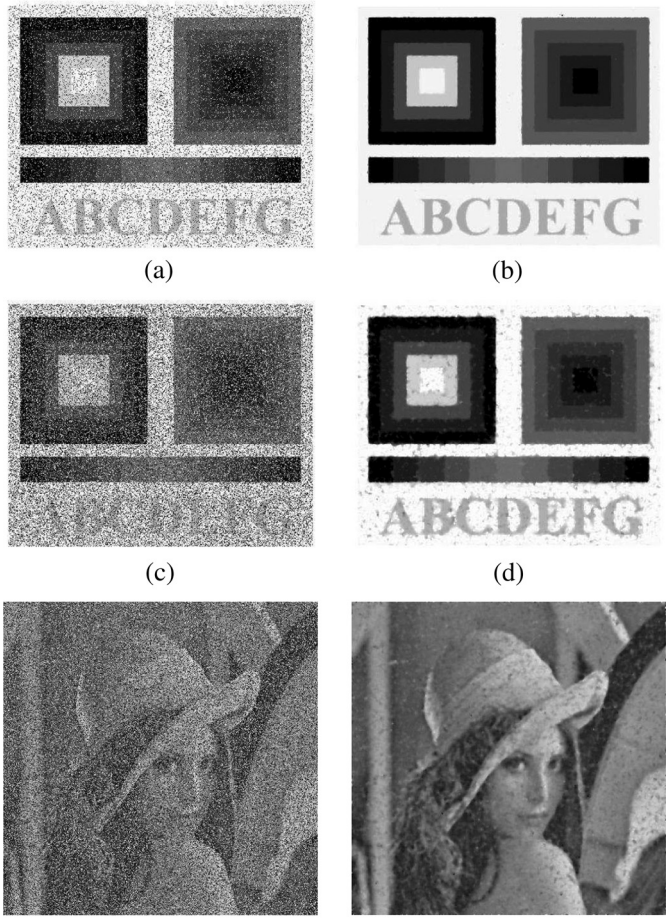

Fig. 1 Denoise results by minimum biased diffusion (MinBAD) method: (a) image with 10% additional noise (PSNR = 15.61 dB); (b) denoised image (PSNR = 34.31 dB, three iterations); (c) image with 50% additional noise (PSNR = 8.60 dB); (d) the denoised image (PSNR = 26.92 dB, five iterations); (e) Lena image with 60% additional noise (PSNR = 11.47 dB); and (f) the denoised Lena image (PSNR = 24.07 dB, five iterations).

additional noise and Figs. 1(b), 1(d), and 1(f) are the corresponding denoised images. In Fig. 1, the peak signal-to-noise ratio (PSNR) is defined as

$$\mathrm{PSNR} = 10\log_{10}\frac{255^2}{\frac{1}{MN}\Sigma_{i=1}^{M}\Sigma_{j=1}^{N}|u(i,j)-u_0(i,j)|^2}, \tag{11}$$

where $u(i,j)$ and $u_0(i,j)$ are the denoised image pixel and original image pixel at (i,j), and M and N are the image width and height. We can see the MinBAD method can remove noise and preserve the edge well for optical images, especially for high-SNR images.

3 Unbiased-Average Minimum Biased Diffusion Approach

From the above filtered images, we can find that the MinBAD approach has excellent denoising ability, and the edge retention is also better. However, if the means of the SAR image blocks change, the radiation resolution and accuracy will change. Our goal is to find a mean-preserving anisotropic diffusion approach for SAR images while denoising. This methodology should retain the radiation relationship between the SAR image and the actual scene.

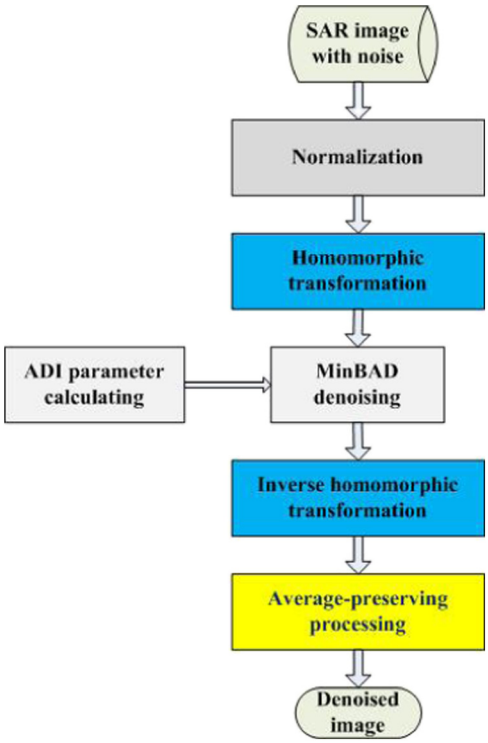

Fig. 2 Unbiased-average MinBAD scheme.

The MinBAD model is also a nonlinear filter. The energy of filtered images is usually not equal to that of the original image. The postapplications of SAR images are mainly based on the image grayscales, which represent the energy of the images. Additionally, the speckle noise is quite different from the general noise of optical images. Based on the basic approach of MinBAD, some improved steps are provided.

Figure 2 presents the improved MinBAD denoise scheme.

The main improving steps are detailed in the following subsections.

3.1 *Normalization*

Because the dynamic range of SAR images is usually very large, in order to improve the denoising approach's generality, normalization is suggested before filtering processing

$$u^0_{\text{normal}} = \frac{u^0}{\max(u^0)}, \tag{12}$$

where u^0 is the original image. The superscripts 0 and n following u here and below represent the discrete time $t = 0$ or $t = n \cdot \Delta t$, where Δt is the iteration time step, and the subscripts normal and ln below following u represent the image data in normalization or logarithm scale.

3.2 *Homomorphic Transformation and Inverse Transform*

The speckle noise of SAR images is multiplicative noise, and the general denoising methods are mostly suitable for additional noise. Logarithm calculation on the normalization image will change the multiplicative noise to additional noise. Also, this homomorphic transformation will compress the dynamic range of the SAR image during the filtering process

$$u^0_{\text{ln}} = \ln(u^0_{\text{normal}} + 1). \tag{13}$$

Here, we add 1 to avoid the negative values in the image $u_{\ln}^0$. Then the denoising processing with the MinBAD approach will be implemented on the image $u_{\ln}^0$. After the anisotropic diffusion on $u_{\ln}^0$, the denoised image is defined as $u_{\ln}^n$. The dataset should be transformed to the original time domain:

$$u_{\text{normal}}^n = \exp(u_{\ln}^n) - 1. \tag{14}$$

3.3 *Average-Preserving Processing*

PDE-based approaches including anisotropic diffusion methods are usually nonlinear algorithms. Therefore, the energy of the processed image is different from that of the original image. In other words, the grayscale will change after filtering. As we know, the grayscale corresponds to the radar cross section of the scene. Therefore, this filtering process will affect the actual radiometry of the SAR image. These filters are average-biased in some sense. In order to decrease the average difference between the original image and filtered image, a mean adjust processing should be added. A detailed approach is as follows. Before the above normalization and logarithm processing, the mean of the original image is calculated and recorded. After filtering processing and inversion of logarithm and normalization processing, we update the mean to the old one. That is

$$u^n = u_{\text{normal}}^n \frac{\text{mean}(u^0)}{\text{mean}(u_{\text{normal}}^n)}. \tag{15}$$

3.4 *Locally One-Dimensional Methods Scheme*

Generally, the numerical solutions of PDEs are implemented by the iterations of differential equations where the iteration efficiency and convergence are very important. According the conclusion of Ref. 15, the alternating direction implicit (ADI)[19] method was recommended instead of the fractional step[20] and additive operator splitting[21] methods for the locally 1-D iteration

$$\begin{cases} \left(1 + \frac{\Delta t}{2} A_1\right) u_{\ln}^* = \left(1 - \frac{\Delta t}{2} A_1 - \frac{\Delta t}{2} A_2\right) u_{\ln}^{n-1} \\ \left(1 + \frac{\Delta t}{2} A_2\right) u_{\ln}^n = u_{\ln}^* + \frac{\Delta t}{2} A_2 u_{\ln}^{n-1} \end{cases}, \tag{16}$$

where $u_{\ln}^*$ is the intermediate image. The two operators A_1 and A_2 are defined as

$$A_1^{n-1} u_{\ln}^n = -|\nabla u_{\ln}^{n-1}| D_x \left(\frac{D_x u_{\ln}^n}{\|\nabla u_{\ln}^{n-1}\|} \right), \tag{17}$$

$$A_2^{n-1} u_{\ln}^n = -|\nabla u_{\ln}^{n-1}| D_y \left(\frac{D_y u_{\ln}^n}{\|\nabla u_{\ln}^{n-1}\|} \right), \tag{18}$$

where D_x and D_y are the differential coefficients along with x and y, respectively.

Usually, the smaller the iteration time step Δt, the more accurate the results and the slower the convergence. Sometimes a proper time step is needed and determined by experimenting. Following Wachspress,[22] a single frequency parameter ξ and the cyclic parameters of length ξ_1 and $\xi_2 (\xi_1 > \xi_2)$ are calculated by the following expressions, respectively:[15]

$$\xi = (\alpha_0 \beta_0)^{1/2}, \tag{19}$$

$$\sqrt{\alpha_1 \beta_1} = \frac{1}{2} \left(\xi_k + \frac{\alpha_0 \beta_0}{\xi_k} \right)^{1/2}, \quad (k = 1,2), \tag{20}$$

where $\alpha_0 = [(\pi/2M)\|A_1\|_\infty]^\delta [(\pi/2M)\|A_1\|_\infty]^{1-\delta}$, M is the length of number of grid points in the x-direction, A_1 is the diffusion operator matrix and the time step 1 can be chosen during the initial A_1 calculation, $\delta \in (0,1)$ is determined by the noise level, $\beta_0 = \|A_1\|_\infty$, $\alpha_1 = \sqrt{\alpha_0 \beta_0}$, and $\beta_1 = \alpha_0 + \beta_0/2$. For the actual SAR image, we cannot obtain the accurate noise parameters

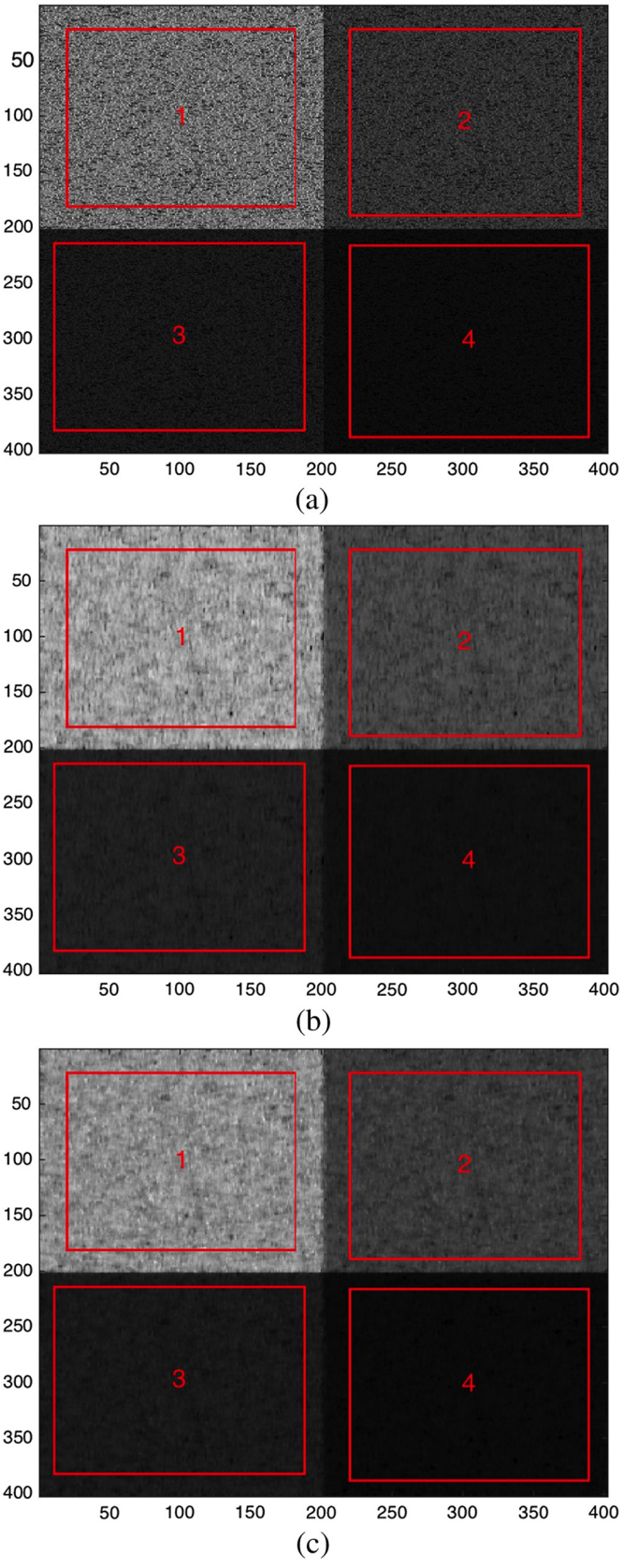

Fig. 3 Simulation results for artificial scene synthetic aperture radar (SAR) image: (a) original image, (b) filtered image via MinBAD approach, and (c) filtered image via unbiased-average MinBAD approach.

such as SNR; however, δ is not sensitive to the time step and it can be calculated approximately by the following expression:

$$\delta = \frac{\mathrm{std}(u_{\mathrm{ln}}^0)}{\max(u_{\mathrm{ln}}^0)}. \tag{21}$$

Then we can obtain the optimum ADI time parameters as follows:

$$\Delta t = 2\xi^{-1}, \tag{22}$$

$$\Delta t_1 = 2\xi_1^{-1}, \quad \Delta t_2 = 2\xi_2^{-1}. \tag{23}$$

The time step calculated by Eq. (22) can be used while the same time step is chosen for Eq. (16), and the different times calculated by Eq. (23) are used for the above equation and the below equation of Eq. (16), respectively. In practice, the iteration of ADI with the above time steps is very fast. Two or three iterations may yield a very small error.

4 Experiments and Analysis

4.1 *Evaluation Indices*

In order to evaluate the speckle denoising effect, three indices including ENL, EPI, and RAE are defined.

ENL is the most common index to describe the noise level for SAR images, and it is defined as

$$\mathrm{ENL} = \frac{\mathrm{mean}^2(u^n)}{\mathrm{var}(u^n)}, \tag{24}$$

where $\mathrm{mean}(u)$ and $\mathrm{var}(u)$ are the mean and variance of the block image u, and u^n is the resultant image after n iterations.

EPI is used to measure the edge preserving ability. In this paper, the definition is

$$\mathrm{EPI} = \frac{\Sigma_{i=1}^{M-1}\Sigma_{j=1}^{N-1}|u_{i+1,j}^n - u_{i,j}^n| + |u_{i,j+1}^n - u_{i,j}^n|}{\Sigma_{i=1}^{M-1}\Sigma_{j=1}^{N-1}|u_{i+1,j}^0 - u_{i,j}^0| + |u_{i,j+1}^0 - u_{i,j}^0|}, \tag{25}$$

where the subscripts i and j indicate the row and column numbers of an image pixel, u^0 is the original image, and u^n is the resultant image after n iterations.

Namely, RAE is used to measure the radiation difference between the filtered image and the original image. RAE is defined as

Table 1 Denoise evaluation indices for artificial scene.

	Original			MinBAD			Unbiased-average MinBAD		
No. of region	ENL	EPI	Mean	ENL	EPI	RAE (dB)	ENL	EPI	RAE (dB)
1	2.849	1	314,340	57.331	0.0724	−0.390	56.873	0.0812	0.018
2	2.845	1	156,860	51.962	0.0816	−0.390	53.013	0.0885	0.012
3	2.846	1	78,510	47.291	0.0909	−0.400	49.020	0.0964	−0.001
4	2.843	1	39,216	42.461	0.1009	−0.407	44.935	0.1052	−0.010

Note: MinBAD, minimum biased diffusion; ENL, equivalent number of looks; EPI, edge preserving index; and RAE, radiation accuracy error.

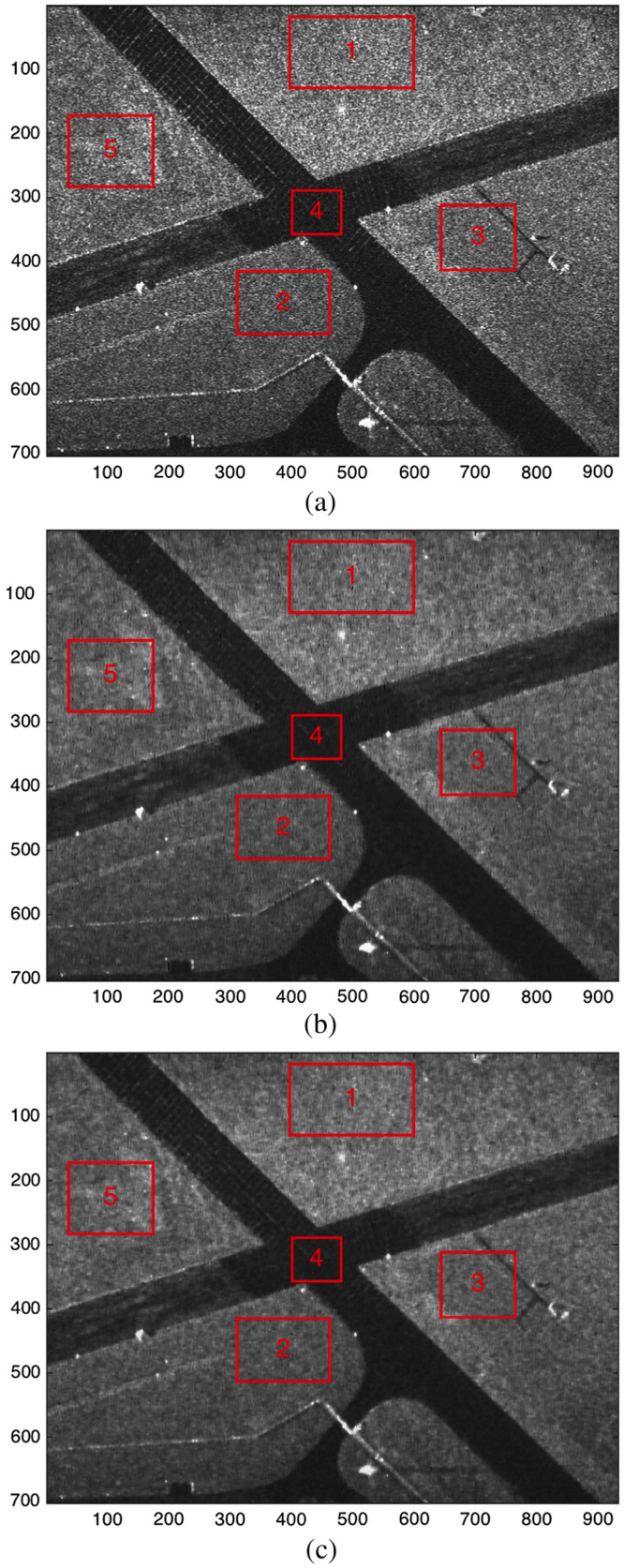

Fig. 4 Simulation results for real SAR image: (a) original image, (b) filtered image via MinBAD approach, and (c) filtered image via unbiased-average MinBAD approach.

$$\mathrm{RAE} = 10\log_{10}\frac{\mathrm{mean}(u^n)}{\mathrm{mean}(u^0)}, \tag{26}$$

where u^0 is the original image, and u^n is the result image after n iterations.

4.2 *Results and Analysis*

Three datasets including an artificial scene and two real SAR images are utilized in this paper. The artificial image is composed of four distributed blocks with different backscatter coefficients and speckle noise. The first real SAR image is an airborne image from spotlight SAR image with 0.6 m resolution from the UK Defence Evaluation and Research Agency enhanced surveillance radar. The second real SAR image is a highspot SAR image from TerraSAR, whose pixel space is 0.5×0.5 m.

Figure 3 illustrates the speckle denoising effect via the MinBAD approach and unbiased-average approach for the artificial scene first. This scene includes four distributed targets, whose means are 8, 4, 2, and 1 times the minimum subimages located in the rightdown position. The evaluation indices for four block images are listed in Table 1.

In Table 1, the means for the original subimages are listed, and the RAEs of the filtered images are listed directly. According to the evaluation indices, we find that the improved approach retains the means for all the gray levels while having good denoising performance. The absolute RAEs of MinBAD are up to 0.390 dB, and those of unbiased-average MinBAD are less than 0.018 dB. In addition, the ENL and EPI indices of the corresponding areas are similar by the two approaches. Comparing to these indices, the excellent RAE is obvious.

Furthermore, Fig. 4 illustrates the speckle denoising effect via the MinBAD approach and unbiased-average MinBAD approach for the real airborne SAR image. And the evaluation indices for five blocks of images are listed in Table 2.

According to Table 2, we find a similar phenomenon as the simulated artificial scene. For this SAR image, the m values of tested subimages range from 2103 to 19,624. The absolute RAEs of MinBAD are greater than 0.369 dB, and those of unbiased-average MinBAD are no more than 0.157 dB. In other words, the unbiased-average MinBAD approach has perfect applicability for different scenarios in average preserving. This approach could be called an unbiased-average approach.

The third experiment illustrates the denoising results on the TerraSAR image in Fig. 5. We also choose five subimages from the image. The evaluation indices for the five blocks of images are listed in Table 3.

According to Table 3, the absolute RAEs of MinBAD are greater than 1.083 dB, and those of unbiased-average MinBAD are no more than 0.267 dB. Additionally, the ENL and EPI indices of our approach are better than those of MinBAD.

For all of the above simulations, two iterations and Eq. (23) were implemented, and the ENL indices are sufficiently high for all the subimages. Thus, we find that the proposed approach has perfect efficiency.

Table 2 Denoise evaluation indices for airborne synthetic aperture radar (SAR) image.

	Original			MinBAD			Unbiased-average MinBAD		
No. of region	ENL	EPI	Mean	ENL	EPI	RAE (dB)	ENL	EPI	RAE (dB)
1	3.268	1	19,624	25.590	0.1165	−0.558	25.341	0.1346	0.015
2	3.523	1	11,599	30.246	0.1249	−0.501	30.195	0.1420	0.062
3	3.132	1	14,394	18.564	0.1268	−0.534	19.090	0.1445	0.029
4	4.083	1	2103	23.698	0.2115	−0.369	24.970	0.2254	0.157
5	2.778	1	18,285	13.143	0.1262	−0.567	12.867	0.1467	0.010

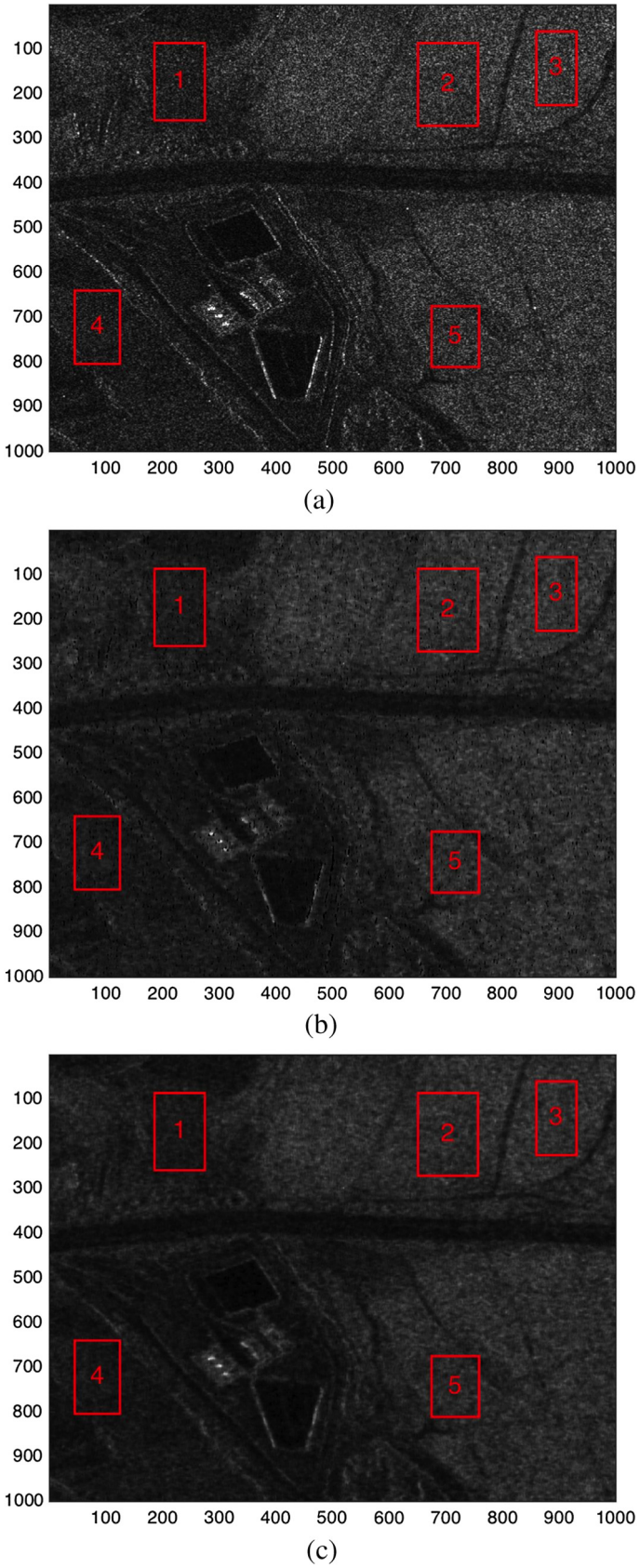

Fig. 5 Simulation results for real TerraSAR image: (a) original image, (b) filtered image via MinBAD approach, and (c) filtered image via unbiased-average MinBAD approach.

Table 3 Denoise evaluation indices for TerraSAR image.

	Original			MinBAD			Unbiased-average MinBAD		
No. of region	ENL	EPI	Mean	ENL	EPI	RAE (dB)	ENL	EPI	RAE (dB)
1	0.691	1	17,020	2.921	0.2683	−1.195	3.623	0.3063	0.124
2	0.903	1	56,785	3.975	0.2087	−1.131	4.568	0.2488	0.226
3	0.989	1	66,865	4.947	0.1917	−1.180	5.718	0.2286	0.187
4	0.795	1	13,725	2.759	0.2882	−1.083	3.284	0.3276	0.254
5	0.959	1	44,813	4.097	0.2114	−1.103	4.665	0.2566	0.267

5 Conclusions

Radiation accuracy is very important for SAR systems and applications. To find a good edge and radiation preserving approach while denoising SAR images, we proposed an improved unbiased-average MinBAD approach for SAR image speckle denoising from the MinBAD method. Three significant steps including normalization, homomorphic transform and inverse transform, and the average-preserving processing are introduced in the unbiased-average MinBAD methods. Also, the RAE index is defined to evaluate average preserving while ENL and EPI are analyzed for speckle denoising. Simulation results demonstrate the effectiveness of the proposed approach for different scenes and different grayscales. The performance of RAE via the unbiased-average MinBAD approach is much better than that of MinBAD.

Acknowledgments

The authors thank Lgence Ltd.'s real spotlight SAR images and Airbus Defense and Space for the highspot TerraSAR image. This work is supported by the National Science Fund of China (61301187 and 61328103).

References

1. J.-S. Lee, "Digital image enhancement and noise filtering by use of local statistics," *IEEE Trans. Pattern Anal. Mach. Intell.* **2**(2), 165–168 (1980).
2. C. Li et al., "Speckle reduction for high resolution one-look space borne SAR images," *Acta Electron. Sin.* **28**(3), 13–16 (2000).
3. A. Baraldi and F. Parmiggiani, "A refined gamma map SAR speckle filter with improved geometrical adaptivity," *IEEE Trans. Geosci. Remote Sens.* **33**(5), 1245–1257 (1995).
4. S. Foucher, G. Benie, and J. M. Boucher, "Multiscale map filtering of SAR images," *IEEE Trans. Image Process.* **10**(1), 49–60 (2001).
5. M. Simard et al., "Analysis of speckle noise contribution on wavelet decomposition of SAR images," *IEEE Trans. Geosci. Remote Sens.* **36**(6), 1953–1962 (1998).
6. F. Argenti and L. Alparone, "Speckle removal from SAR images in the undecimated wavelet domain," *IEEE Trans. Geosci. Remote Sens.* **40**(11), 2363–2374 (2002).
7. H. Xie, L. E. Pierce, and F. T. Ulaby, "SAR speckle reduction using wavelet denoising and Markov random field modeling," *IEEE Trans. Geosci. Remote Sens.* **40**(10), 2196–2212 (2002).
8. T. Chan and J. Shen, *Image Processing and Analysis: Variational, PDE, Wavelet, and Stochastic Methods*, SIAM, Philadelphia, Pennsylvania (2005).
9. P. Perona and J. Malik, "Scale-space and edge detection using anisotropic diffusion," *IEEE Trans. Pattern Anal. Mach. Intell.* **12**(7), 629–639 (1990).
10. P. Perona, T. Shiota, and J. Malik, "Anisotropic diffusion," in *Geometry-Driven Diffusion in Computer Vision*, pp. 73–92, Springer, Utrecht, The Netherlands (1994).

11. J. Weickert, *Anisotropic Diffusion in Image Processing*, Vol. 1, B. G. Teubner, Stuttgart, Germany (1998).
12. Y. Chen, C. A. Z. Barcelos, and B. A. Mair, "Smoothing and edge detection by time-varying coupled nonlinear diffusion equations," *Comput. Vision Image Understanding* **82**(2), 85–100 (2001).
13. Y. Yu and S. T. Acton, "Speckle reducing anisotropic diffusion," *IEEE Trans. Image Process.* **11**(11), 1260–1270 (2002).
14. S. Kim, I. E. Iacob, and M. Tynan, "Minbad: the minimum-biased anisotropic diffusion for noise removal," Technical Report 02-06, University of Kentucky, Lexington (2002).
15. K. Joo and S. Kim, "PDE-based image restoration, I: antistaircasing and anti-diffusion," Technical Report 2003-07, University of Kentucky, Lexington (2003).
16. K. Joo and S. Kim, "PDE-based image restoration, II: numerical schemes and color image denoising," Technical Report 2003-08, University of Kentucky, Lexington (2003).
17. S. Kim, "PDE-based image restoration: a hybrid model and color image denoising," *IEEE Trans. Image Process.* **15**(5), 1163–1170 (2006).
18. V. S. Frost et al., "A model for radar images and its application to adaptive digital filtering of multiplicative noise," *IEEE Trans. Pattern Anal. Mach. Intell.* **4**(2), 157–166 (1982).
19. J. Douglas, Jr., "On the numerical integration of $[(\partial^2 u/\partial x^2) + (\partial^2 u/\partial y^2)] = (\partial u/\partial t)$ implicit methods," *J. Soc. Ind. Appl. Math.* **3**(1), 42–65 (1955).
20. E. D'yakonov, "Difference schemes with split operators for multidimensional unsteady problems (English translation)," *USSR Comp. Math.* **3**, 581–607 (1963).
21. J. Weickert, B. T. H. Romeny, and M. A. Viergever, "Efficient and reliable schemes for nonlinear diffusion filtering," *IEEE Trans. Image Process.* **7**(3), 398–410 (1998).
22. E. L. Wachspress, "Optimum alternating-direction-implicit iteration parameters for a model problem," *J. Soc. Ind. Appl. Math.* **10**(2), 339–350 (1962).

Bing Sun received his BS and PhD degrees from Beihang University, China, in 2003 and 2008, respectively. He was a postdoctorate after 2008. Currently, he has been with the School of Electronics and Information Engineering, Beihang University, since 2010. From November 2013 to November 2014, he was a visiting scholar in the Department of Mathematics, University of Texas-Pan American. His current activities are synthetic aperture radar system design, imaging algorithm, and image processing.

Jie Chen received his BS and PhD degrees in information and communication engineering from Beihang University, China, in 1996 and 2002, respectively. From 2009 to 2010, he was a visiting researcher with the School of Mathematics and Statistics, University of Sheffield, United Kingdom. Currently, he is with the School of Electronics and Information Engineering, Beihang University, where he has been a full professor since 2011. His current research interests include data fusion, topside ionosphere exploration, and so on.

Eric Tovar received his BS degree in applied mathematics at the University of Texas-Pan American in 2013. He has been an MS student in the Department of Mathematics at the University of Texas-Pan American since 2013. His current research interest is nonlinear partial differential equations.

Zhijun Qiao received his PhD degree in applied mathematics from the Institute of Mathematics, Fudan University, China, in 1997. From 1999 to 2001, he was a Humboldt research fellow at the University of Kassel, Germany. From 2001 to 2004, he was a researcher in Los Alamos National Laboratory. Currently, he is with the Department of Mathematics, University of Texas-Pan American. His research interests include nonlinear partial differential equations and their application in radar imaging.